Rovibrational eigenenergy structure of the [H,C,N] molecular system

Georg Ch. Mellau[a)]

Physikalisch-Chemisches Institut, Justus-Liebig-Universität Giessen, Heinrich-Buff-Ring 58,
D-35392 Giessen, Germany

The vibrational-rotational eigenenergy structure of the [H,N,C] molecular system is one of the key features needed for a quantum mechanical understanding of the HCN⇌HNC model reaction. The rotationless vibrational structure corresponding to the multidimensional double well potential energy surface is well established. The rotational structure of the bending vibrational states up to the isomerisation barrier is still unknown. In this work the structure of the rotational states for low and high vibrational angular momentum is described from the ground state up to the isomerisation barrier using hot gas molecular high resolution spectroscopy and rotationally assigned *ab initio* rovibronic states. For low vibrational angular momentum the rotational structure of the bending excitations splits in three regions. For $J < 40$ the structure corresponds to that of a typical linear molecule, for $40 < J < 60$ has an approximate double degenerate structure and for $J > 60$ the splitting of the e and f components begins to decrease and the rotational constant increases. For states with high angular momentum, the rotational structure evolves into a limiting structure for $v_2 > 7$ – the molecule is locked to the molecular axis. For states with $v_2 > 11$ the rotational structure already begins to accommodate to the lower rotational constants of the isomerisation states. The vibrational energy begins to accommodate to the levels above the barrier only at high vibrational excitations of $v_2 > 22$ just above the barrier whereas this work shows that the rotational structure is much more sensitive to the double well structure of the potential energy surface. The rotational structure already experiences the influence of the barrier at much lower energies than the vibrational one. © *2011 American Institute of Physics*. [doi:10.1063/1.3590026]

I. INTRODUCTION

Fundamental understanding of the structure and dynamical evolution of molecules can be extracted from high resolution spectra. The list of possible rovibrational eigenenergies is the main result obtained from these experiments. In principle, these eigenenergies could be determined to any precision by theoretical calculations if the molecular Schrödinger equation, which describes the correlated motions of the electrons and nuclei could be solved exactly. This is, however, not possible, because while this multi-dimensional eigenvalue differential equation is extremely simple to formulate, it is impossible to solve. For polyatomic molecules we can obtain theoretical eigenenergies for the molecular motion of the nuclei only within the Born-Oppenheimer approximation using a highly accurate potential energy surface (PES). But even using such an exact PES the eigenenergies observed do not reach the accuracy of the high resolution experiments. In fact in high resolution spectroscopy we reverse the situation described: we use experiments to solve the molecular Schrödinger equation. The analysis of the observed line positions reveals the eigenenergy structure; the analysis of the line intensities gives direct information about the wave functions. From a theoretical point of view they are strongly correlated through the assigned quantum numbers.

Molecular vibrations and rotations are well understood at low excitation energies around the equilibrium structure but if the molecule gains energy in a quantity relevant to chemical reactions there are still many open questions. H_2O, H_3^+ Acetylene, HCP, and HCN/HNC are the model molecules for which experimental and theoretical studies have been done at the most basic level. The HCN and HNC isomers correspond to two global minima of the [H,C,N] molecular system with the two stable linear isomers HCN and HNC. This system is important because there is an overlap between the two basic scientific tools that we can use to gain a fundamental understanding of molecular physics on a full quantum mechanical basis. It is possible to do high-level *ab initio* theoretical calculations (only 17 particles) and high resolution spectroscopic data can be obtained for highly excited rovibrational states. The isomerisation reaction HCN⇌HNC is one of the important model systems for the study of unimolecular reactions. Figure 1 shows the one dimensional PES of the molecular system along the isomerisation path as the hydrogen atom bends from one side of the CN core to the other. To describe the relative positions of the nuclei in HCN and HNC the Jacobi coordinates (R,r,γ) are used: $R = r_{H-CN}$ is the distance between the H atom and the center-of-mass of the molecule CN part, $r = r_{CN}$ is the distance between the N and C atoms and γ the angle between R and the CN bond axis. On the HCN–HNC potential curve, the γ coordinate varies linearly between the HCN ($\gamma = 0$) and HNC ($\gamma = \pi$) structures.

[a)]Electronic mail: georg@mellau.de. URL:http://www.georg.mellau.de.
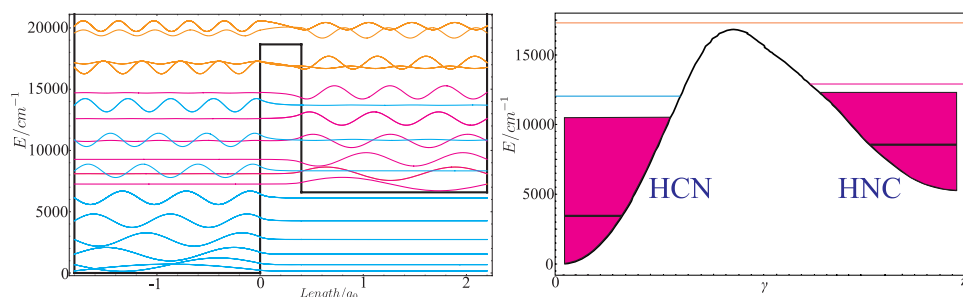
134, 194302-1

FIG. 1. Schematic one-dimensional solutions for the asymmetric double minimum potential. Left: for the one dimensional square double well (Ref. 1). The blue and red wavefunctions are localized in one of the two wells, the orange ones correspond to both minima. Right: the [H,C,N] molecular system, only the dimension along the isomerisation path is shown (Ref. 2). The red area marks the eigenenergy regions where all 3822 and 1191 eigenenergies, respectively, have been measured.

To understand how the HCN and HNC molecules behave when they become highly excited, we need to determine the complete vibrational-rotational eigenenergy level structure of the [H,C,N] molecular system. Figure 1 shows the eigenenergies and wavefunctions for the simplest model we can define for the [H,C,N] molecular system: the asymmetric infinite square double well potential. The wavefunctions below the barrier are localized in one of the two wells, and the wavefunctions above the barrier correspond to both minima. We have a similar situation for the [H,C,N] system. The eigenenergies and wavefunctions below the barrier are localized in one of the two wells and correspond to the two separate molecules HCN and HNC; the ones above the barrier belong to a single "combined" $H_{0.5}$–CN–$H_{0.5}$ molecule.[3] Our simple model in Fig. 1 reveals the basic feature of such a double well potential: the lower eigenenergies on both sides are independent of one another, but that already begins to change before the energy reaches the barrier height. For the [H,C,N] molecular system we have a similar multidimensional problem; the one dimensional double well PES shown in Fig. 1 is only an approximation even for pure bending vibrations.

II. HOTGAME SPECTROSCOPY OF THE [H,C,N] MOLECULAR SYSTEM

In hot gas molecular emission (HOTGAME) spectroscopy a molecular gas is heated to high temperatures, and the infrared emission is collected with a high resolution spectrometer. HOTGAME spectroscopy was pioneered by Peter Bernath[4] mainly to record the high resolution spectra of short-lived diatomic molecules. HOTGAME spectroscopy can be used to detect the highly excited rovibrational bending states of small molecules with a very high sensitivity. There are two reasons for the high sensitivity of this often ignored experimental scheme: one is due to the physics of transitions in a hot molecular gas[5] and the other to the sensitivity of the FTIR spectrometers used to record the spectra. Using HOTGAME, highly excited states of H_2O,[6–8] HCN,[9–13] and HNC (Refs. 5, 14, and 15) isotopologues have been successfully measured and analyzed.

To cover all eigenenergies of the molecular system, not only highly excited vibrational states, but also rotationally excited states have to be determined. Using HOTGAME spectroscopy it may be possible to cover all of the approximately

45 000 states of the [H,C,N] system up to the isomerisation barrier. In two recent papers such a complete eigenenergy study for the HNC isotopomer has been reported[5,15] for the lower rovibrational excitation energy range where the theoretical description of the eigenstates through perturbation methods still holds. In this paper we report the results for low and high angular momentum states from a similar analysis done for HCN and compare the results to the ones obtained for HNC. The results for all detected l sublevels are published in two separate papers.[16,17] For HNC and HCN we extended the analysis to higher excited states than reported in the previous papers. The experimental results are given as supplementary material to this paper;[18] the list of the vibrational states and the determined spectroscopic constants are listed in Table I. Eigenenergy values are given as term values in cm^{-1}.

The linear HCN and HNC molecules have three normal modes $v = v_1, v_2, v_3$ two stretching vibrations of Σ^+ symmetry and a bending mode of Π symmetry: v_1 is the HN stretch at 3311.47/3652.65 cm^{-1}, v_3 is the CN stretch at 2096.84/2023.86 cm^{-1}, and v_2 is the degenerate bending mode at 711.97/462.72 cm^{-1}. The rovibrational eigenstates are labeled using the quantum numbers of the Wang symmetrized basis functions $|v, l, J, (e/f)\rangle$, where l is the vibrational angular momentum quantum number and J the end-over-end rotational quantum number. We use the symmetry labels e and f as the possible values of a symbolic quantum number e/f labeling the eigenvalues. For a linear molecule the vibrational angular momentum l is the only contribution to the axial component of the angular momentum. The vibrational angular momentum is equal to the absolute value of the signed quantum number k in the symmetric top basis functions $l = |k|$.

To show the rotational effects described in this paper the experimentally determined rovibrational eigenenergy corresponding to each vibrationally excited state is plotted using a reduced energy value E_r by subtracting two terms $E_{v,(J=0)}$ and $E_{0,J}$ from each measured value

$$E_r = E_{meas} - E_{v,(J=0)} - E_{0,J}. \qquad (1)$$

$E_{v,(J=0)}$ is the rotationless vibrational energy calculated for $l \neq 0$ vibrational states by extrapolating the rotational states to the nonphysical $J = 0$ state. This term value is constant for the rotational manifold corresponding to a given (v_1, v_2, l, v_3) vibrational substate and describes the basic

contribution of the vibration to the rovibrational eigenenergies. In an excited bending state, the rotating linear molecule has an effective moment of inertia and a component of angular momentum about the figure axis. In an excited bending mode, the linear molecule is therefore a symmetric top and the rotational energy values are to the first approximation[19]

$$B_v J(J+1) + (A_v - B_v)l^2. \qquad (2)$$

The eigenenergy due to the vibrational angular momentum is usually divided in two components, the $A_v l^2$ positive component is treated as vibrational energy and the $-B_v l^2$ negative component is treated as rotational energy. This splitting is necessary for practical purposes: due to this splitting the vibrational dependence of the rotational constant is not included in the vibrational energy. If the analysis of the rovibronic eigenenergies is completed, it is possible to redefine the vibrational energy and to include the $-B_v l^2$ term. Alternatively, we can use the experimental eigenenergy values for a (v_1, v_2, l, v_3) vibrational substate and interpolate the eigenenergies to $J = 0$. The $E_{v,(J=0)}$ vibrational eigenenergies used in this work have been calculated through such an interpolation of the parity component with the lower eigenenergy value using the eigenenergies up to $J = 30$. The $E_{v,(J=0)}$ vibrational eigenenergies are approximately equal to the eigenenergy values predicted for $J = 0$ by the physical model defined in Ref. 16 (sometimes denoted G_c or $T_{v,J=0}$). For the states reported here the difference between these two definitions is less than 0.01 cm^{-1}. The $E_{v,(J=0)}$ vibrational eigenenergy allows us to visualize the vibrational, rotational, and rotation-vibration interaction effects with increasing rotational excitation relative to the zero order situation for a (v_1, v_2, l, v_3) vibrational substate.

$E_{0,J}$ energy values correspond to the vibrationless ground state and describe the manifold of the rotational states in the case where the molecule is not vibrating. This is not only a visual scaling of the eigenenergy values but also a physical one: We consider the difference between the rotational manifold in a vibrating state relative to all rotational effects that we observe at high rotational excitations in the vibrationless state. The reduced energy E_r is plotted against the J quantum number for each e/f symmetry label. We plot against J rather than $J(J+1)$ (which is equivalent to plot against rotational excitation energy) because the true independent variable of the problem is the J quantum number and not the rotational energy value. With the definition of $E_{v,(J=0)}$ used in this work the reduced energy plots are defined only through the exact Schrödinger equation and are meaningful for the isomerisation states.

III. APPROXIMATE TWOFOLD ROTATIONAL DEGENERACY OF THE HCN AND HNC ROVIBRATIONAL STATES WITH LOW ANGULAR MOMENTUM

Figures 2 and 3 show the evolution of the rovibrational eigenenergy for HCN and HNC with increasing rotational quantum numbers for low angular momentum excitations. The eigenenergies shown fit the classical expressions used to describe the rotational-vibrational eigenenergies of a linear

molecule extremely accurately. The curves shown in Figs. 2 and 3 reveal interesting molecular physics behind the interplay of the high order spectroscopic constants.

For the bending vibrational states with $l = 0$ and 1 angular momentum we report here an approximate twofold rotational degeneracy at high rotational excitation $(60 > J > 40)$. For which of the two vibrational states the rotational eigenenergy becomes approximately the same is different between HCN and HNC. Such difference is not surprising since the curvature of the bending potentials is quite different for the two molecules (with considerably different bending frequencies). The two (e, f) components of the rovibrational eigenenergy are the two degenerate components of the bending vibrational excitation in the harmonic approximation of a nonrotating linear molecule. The degeneracy is lifted in a rotating molecule by $\Delta l = \Delta k = \pm 2$ Coriolis matrix elements connecting substates with different angular momentum, the separation between the levels increases with the rotational excitation.[20,21] The matrix element is proportional to v_2 and J, the splitting in the e and f components should increase with bending excitation for the same rotational quantum number. This is what we observe experimentally for low $(J < 40)$ vibrational excitation.

At high rotational excitation $(J > 40)$ the evolution of the eigenenergies is determined by several effects. There is a distinguished plane formed by two spatial directions: the molecule axis and the direction of rotational angular momentum. We expect that the two degenerate components of the bending vibration will be separated into two nondegenerate vibrations: one vibration in the distinguished plane and one perpendicular to it. The corresponding classical picture correlates with the two different rotational structures. The Coriolis force depends on the angle between the axis of rotation and the vibrational velocity of the molecules in an axis frame fixed to the molecule. The Coriolis force for the vibration in the spatially distinguished plane is zero, and for the vibration perpendicular to it, it has a maximum value. If for a linear molecule the bending mode is excited, the rovibrationally averaged angle γ in these bound states $\gamma = \langle \gamma \rangle = \langle \Psi | \gamma | \Psi \rangle$ is not 0. $\langle \gamma \rangle$ is increasing substantially with the bending excitation so that at high excitation of the bending vibration, the linear molecule can be considered as a slightly asymmetric rotor.[23] The rotational energy levels for a slightly asymmetric rotor[22] for $K_a = 0$ and 1 show a similar evolution at high J as observed here for HCN and HNC. With rotational excitation, the off-diagonal matrix elements connecting the sublevels with different vibrational angular momentum increase continuously and l loses its significance as quantum number.

For HCN the e states with zero or one vibrational angular momentum the rotational eigenenergy in the excited bending states corresponds approximately to the rotational structure of the non-vibrating molecule plus a constant energy factor, which increases approximately with $\Delta E = 3.6(7)$ cm^{-1} as the bending excitation increases

$$E_{v,J} = E_{v,J=0} + E_{0,J} + m \times \Delta E \quad \text{for} \quad 40 < J < 60. \quad (3)$$

This may be interpreted as a decoupling of the rotation from the vibration. The separations between the flat

TABLE I. State term value matrix constants in cm^{-1}. The uncertainty in the last digits (standard deviation) is given in parenthesis. Values that do not have any uncertainty are calculated values and have been fixed in the fit.

| Nr.	State	$T_v(J=0)$	$G_{vs}(v,l)$	B_v	D_v10^6	H_v10^{12}	q_v10^3	q_v10^8	$q_{v,J}10^{12}$	ρ_v10^8	$q_{lv}10^4$	J_m
						HNC						
1	08^00	3743.7	3743.76413	1.5629262	2.8565	53.38	11.926(17)	34.56(76)	19.5	−11.21	0.1635	
2	08^20	3758.8	3765.01125	1.5602499	4.3307	41.29						
3	08^40	3803.7	3828.61534	1.5529377	4.0833	−79.75						
4	08^60	3879.5	3935.04181(25)	1.5404861(25)	3.2974(314)	−101.10						30
5	08^80	3986.1	4083.70656(28)	1.5239014(24)	2.9510(131)	−169.21(614)						44
6	09^10	4210.1	4211.47014	1.5688808	4.4238	78.12	13.300	28.49	19.5	−11.21	0.1635	
7	09^30	4241.0	4255.46836	1.5639072	4.1381	48.65						
8	09^50	4304.4	4343.30447	1.5538707	4.6714	−10.27						
9	09^70	4399.9	4475.30106(59)	1.5389000(20)	3.6551(51)	−190.00						30
10	09^90	4528.1	4651.21748(49)	1.5196393(39)	3.0747(15)	−366.62						40
11	18^00	7205.2	7205.15609	1.5573204	4.9764	90.72	12.920(162)	71.60	14.5	−8.708	0.0021	
12	18^20	7220.1	7226.04366	1.5533536	6.9728	73.51						
13	18^40	7264.1	7288.73388	1.5467063	5.9982	21.89						
14	18^60	7338.2	7393.48112(74)	1.5332604(56)	2.9520(1440)	−64.13						25
15	18^80	7442.8	7539.82161(48)	1.5157180(37)	2.6400(838)	60.60(713)						43
						HCN						
16	010^00	6855.4	6855.44308	1.5214816	3.7082	27.52	8.65	16.00	3.8	−2.071	0.0656	50
17	010^20	6871.3	6877.35279	1.5205751	3.7273	15.94						
18	010^40	6918.6	6942.97375	1.5175444	3.6620	12.49						
19	010^60	6997.5	7052.02182	1.5124933	3.5530	6.73						
20	010^80	7107.5	7203.92670	1.5054217	3.4005	−1.33						
21	$010^{10}0$	7248.4	7398.03672(18)	1.4955542(7)	3.2210(7)	−26.99(20)						
22	011^10	7515.8	7517.26334	1.5268450	3.6497	18.74	8.75	16.50	4.0	−2.071	0.0828	
23	011^30	7547.4	7561.33259	1.5248307	3.5908	16.43						
24	011^50	7611.3	7649.36549	1.5208021	3.4729	11.83						
25	011^70	7706.6	7780.90083	1.5147593	3.2960	4.91						
26	011^90	7833.2	7955.32179	1.5067022	3.0602	−4.29						
27	$011^{11}0$	7990.9	8171.83419(19)	1.4944571(12)	3.2005(21)	−67.81(101)						40
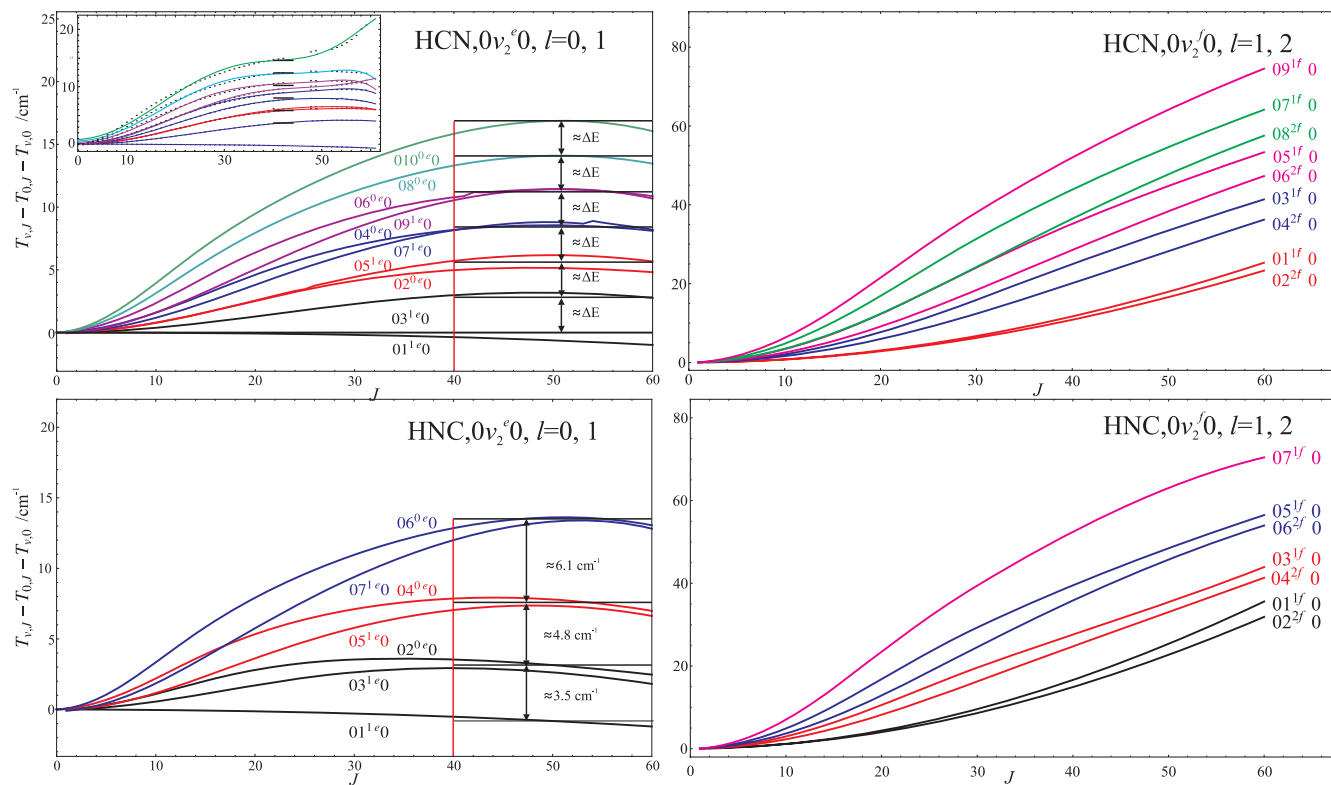
FIG. 2. The evolution of the reduced rovibrational eigenenergy for the HCN and HNC ν_2 states with zero or single vibrational angular momentum excitation with increasing bending excitation.
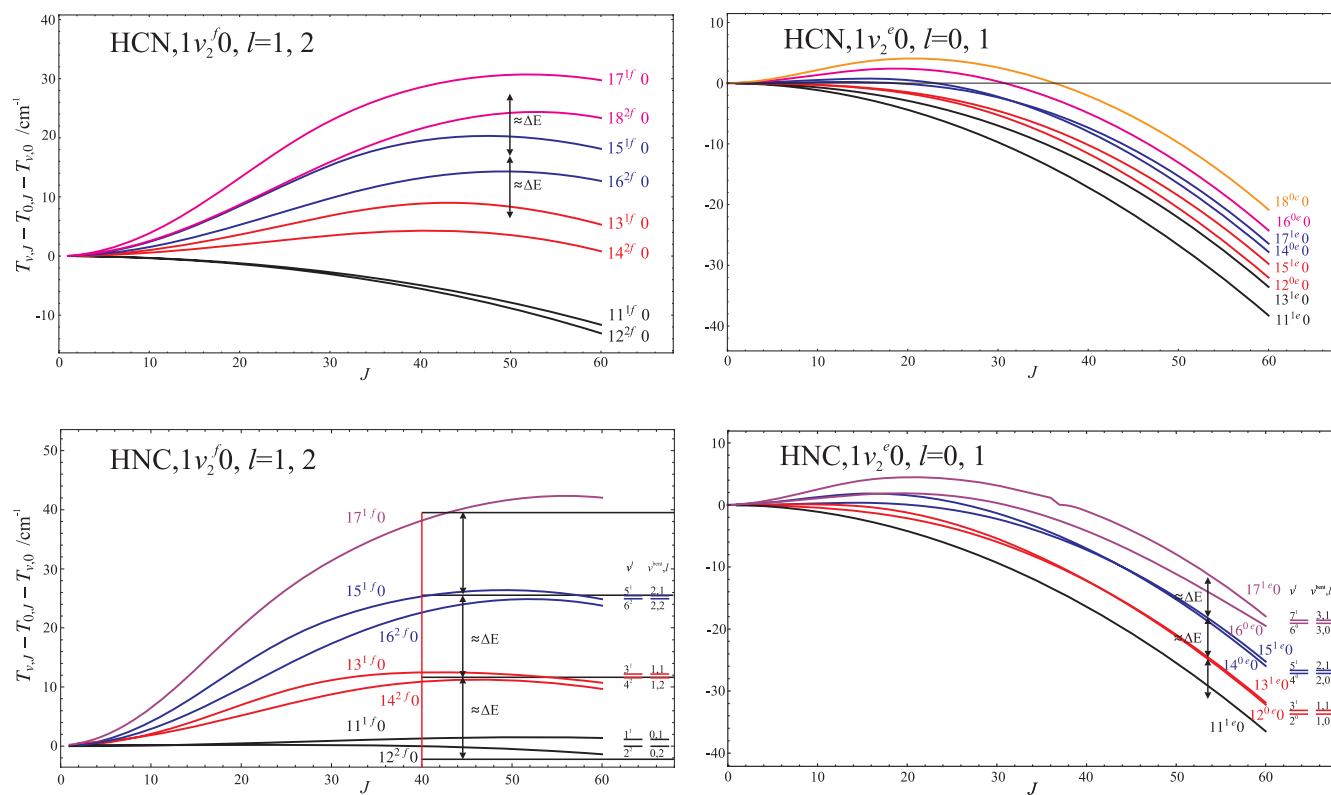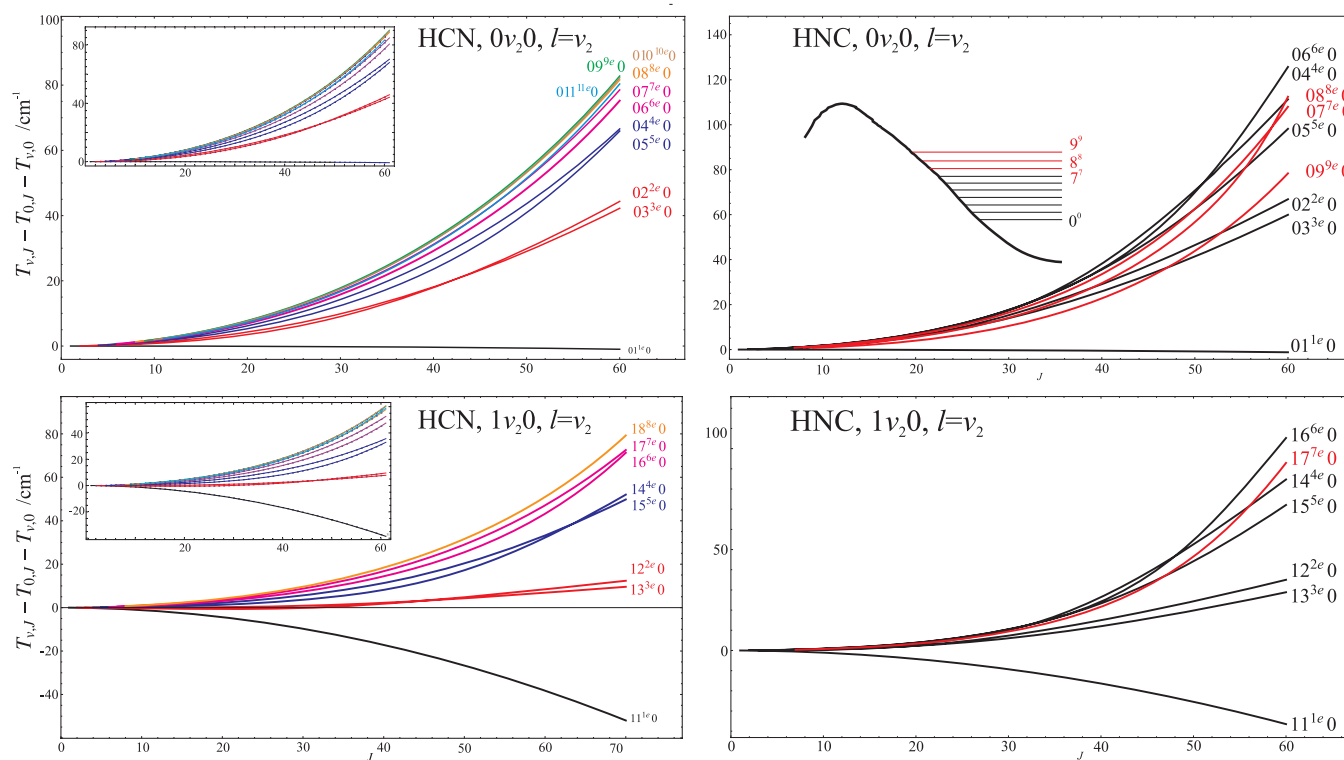

FIG. 3. The evolution of the reduced rovibrational eigenenergy for the HCN and HNC $\nu_1 + \nu_2$ states with zero or single vibrational angular momentum excitation with increasing bending excitation.

FIG. 4. The evolution of the reduced rovibrational eigenenergy for the HCN and HNC ν_2 states with highly excited vibrational angular momentum with increasing bending excitation.

eigenenergy regions match the $g_{22} = 3.76(1)$ cm^{-1} parameter for $E_{v,J=0}$ vibrational energies calculated for pure bending states. The f states with $l = 1, 2$ also have an equidistant structure, but it is less pronounced than for the e states. The eigenenergy structure described is valid only for rotational excitations in the range of $40 < J < 60$, for higher excitations the effects corresponding to the double well potential change this structure. The eigenenergy lists determined experimen-

tally in this work reach up to $J = 85$, and there is a clear trend for rotational excitations with $J > 60$, the effective e/f splitting is decreasing with rotational excitation.

The experimental study presented here does not reach up to the barrier of isomerisation. To understand the eigenenergy structure it is necessary to use values from *ab initio* calculations. In fact all 45 000 eigenvalues up to the isomerisation barrier have already been calculated.[24,25] For the [H,C,N]

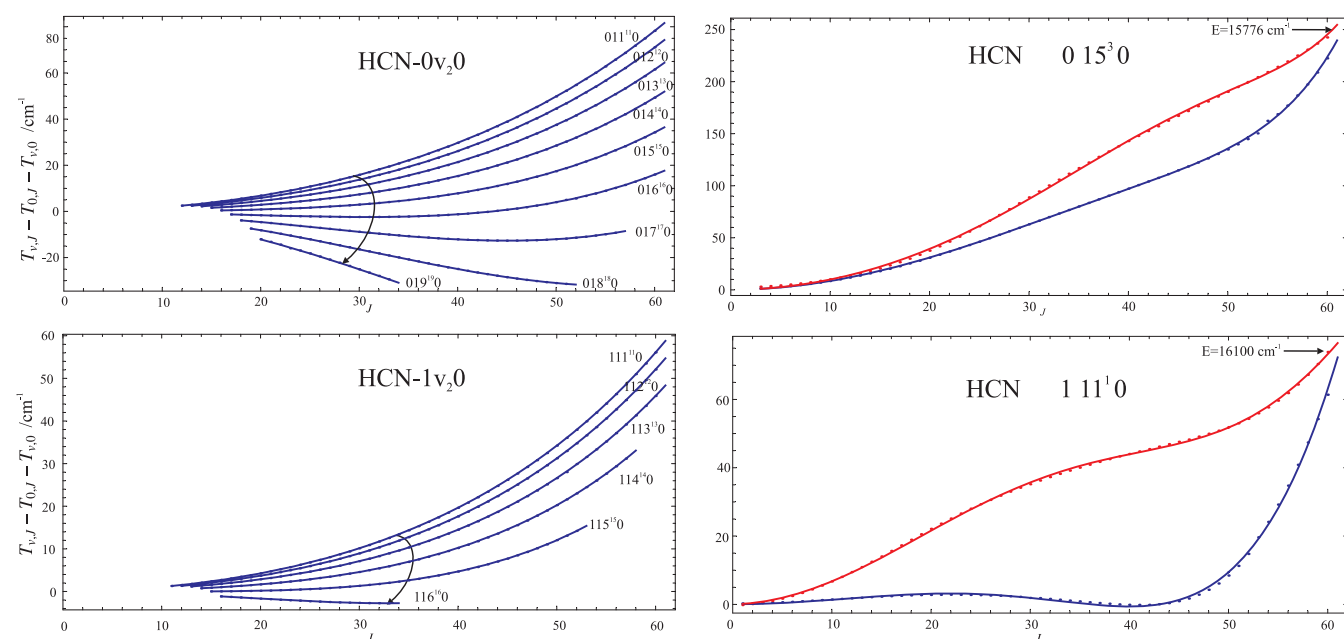FIG. 5. Typical variation of the l-doubling for HCN and HNC up to the isomerisation barrier. Upper left figure: The evolution of the reduced rovibrational eigenenergy for the HCN states with highly excited vibrational angular momentum.
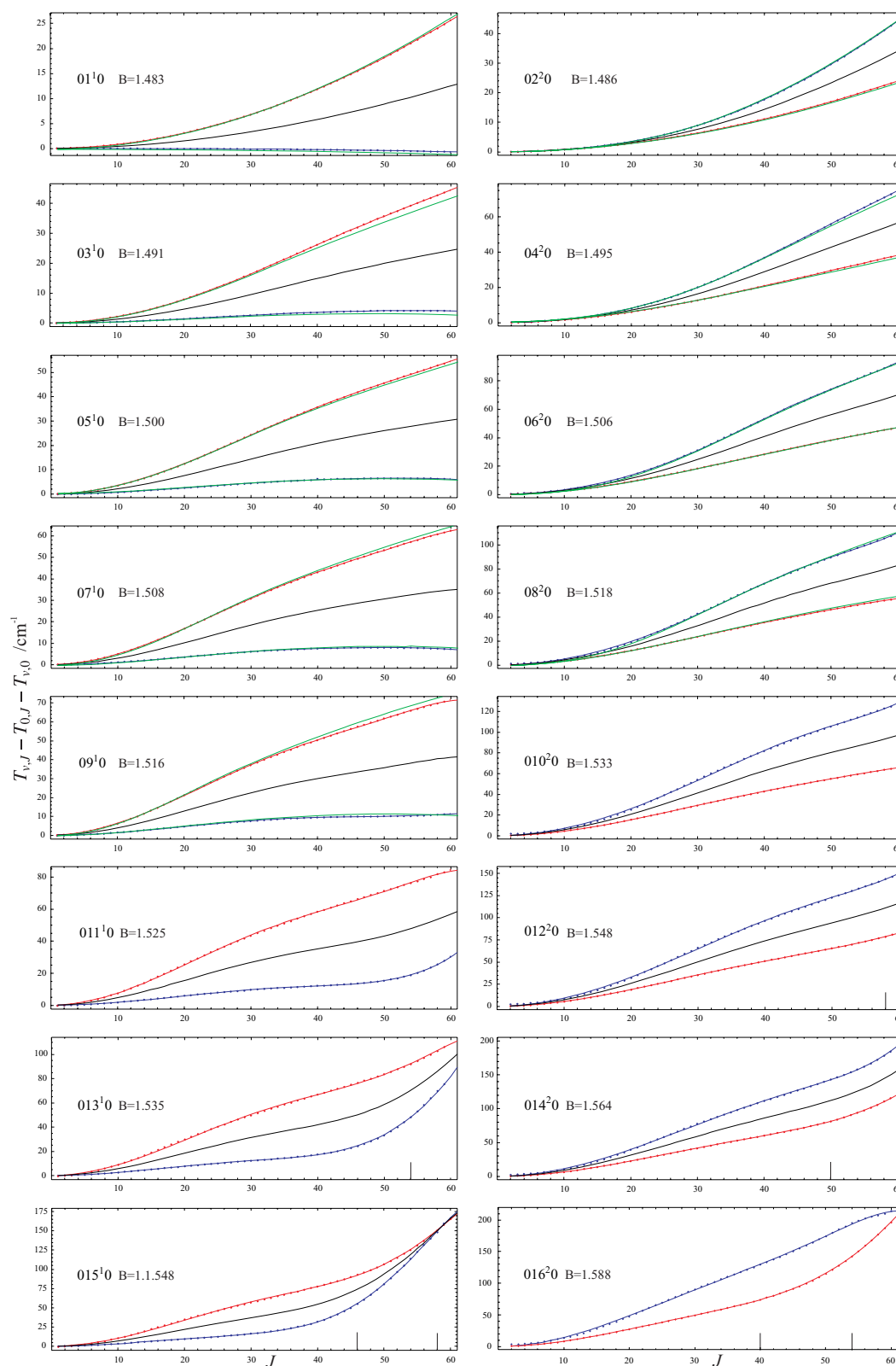
FIG. 6. The evolution of the reduced rovibrational eigenenergy for the HCN bending states up to the isomerisation barrier. The $E_{v,(J=0)}$ vibrational energy used to calculate the reduced energy was calculated from the *ab initio* data. (blue: e states; red: f states; green: experimental eigenenergies relative to the experimental $E_{v,(J=0)}$ vibrational energy; first vertical line: barrier height mark; second vertical line: barrier height plus 2000 cm^{-1}).
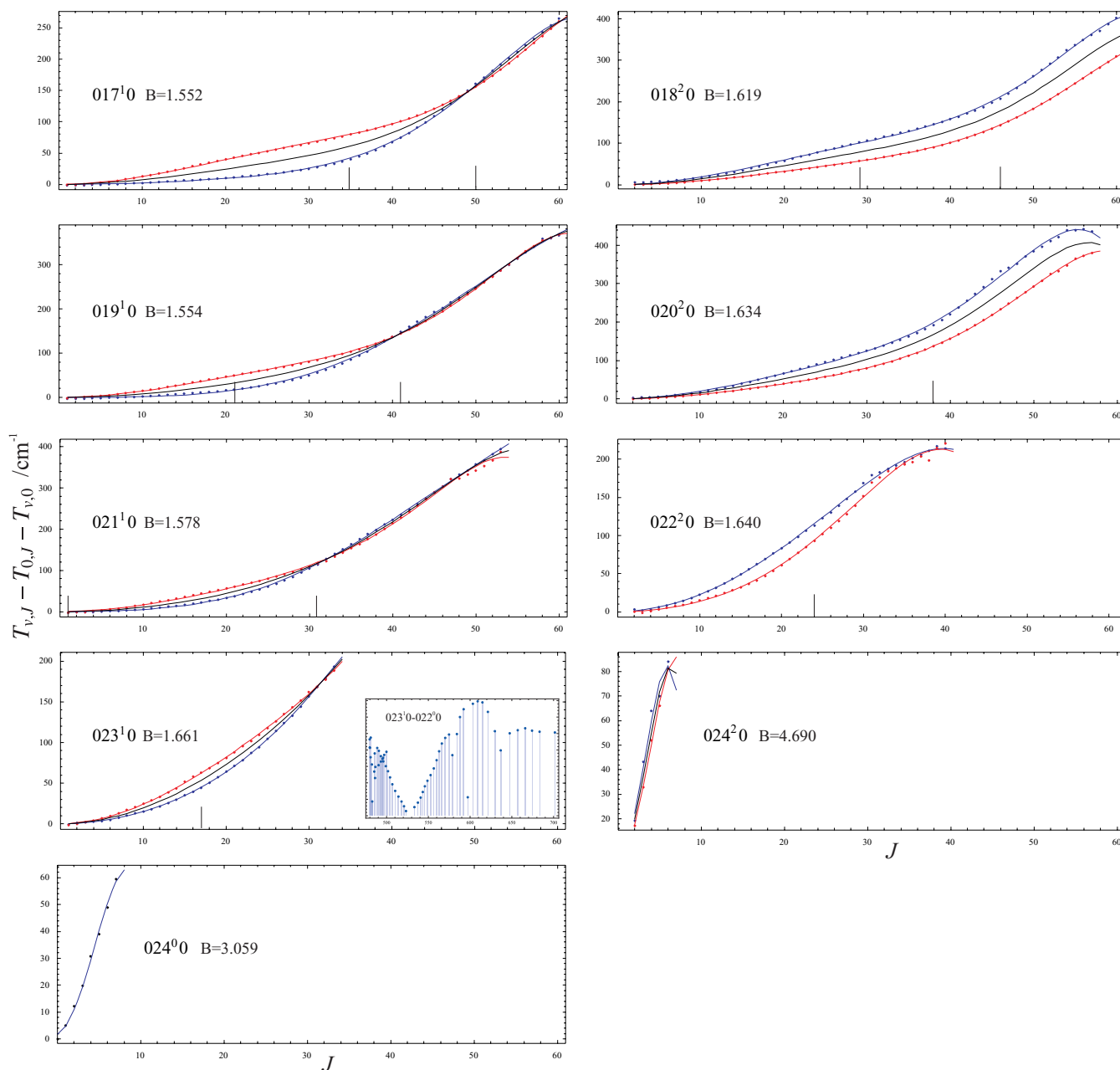
FIG. 7. The evolution of the reduced rovibrational eigenenergy for the HCN bending states up to the isomerisation barrier; the inset represents a simulated emission spectrum for 2000 K (blue: e states; red: f states; first vertical line: barrier height mark; second vertical line: barrier height plus 2000 cm^{-1})

molecular system only parity and total angular momentum are exact quantum numbers and the eigenenergies have to be labeled with vibrational quantum numbers in an assignment procedure. This work presents the results from the rotational assignment of all rovibrational eigenenergies up to the isomerisation barrier. The eigenenergies published in Ref. 25 have been used for this analysis. When the assignment work was started there was no reason to try to construct a better PES and to recalculate the rovibrational eigenenergies. For the HNC part of the potential the HOTGAME results show that the eigenenergies and the conclusions that we get from such a study may differ for a more accurate PES. For the HCN part of the potential and for the main features of the eigenenergy structure around the isomerisation barrier the eigenenergy list should give us definitive results. The vibrational assignment

can be done using either the wave functions[26] or the rotational structure of the eigenenergies as assignment information. The assignment reported here is based on the rotational structure. The assignment was done by assuming that the eigenenergies are described by spectroscopic constants up to the isomerisation and that the eigenenergy structure is not disturbed by quantum monodromy,[27] details of the assignment procedure can be found in Ref. 16.

For the low l states the inset in Fig. 2 shows approximately the same rotational structure as detected in the experiment. Figure 5 shows some typical rotational structures for low l states up to the isomerisation barrier: the e and f components of the doublets begin to move closer together and just before the barrier the slope of the eigenenergy curve increases substantially. Figures 6 and 7 show the step by step evolution
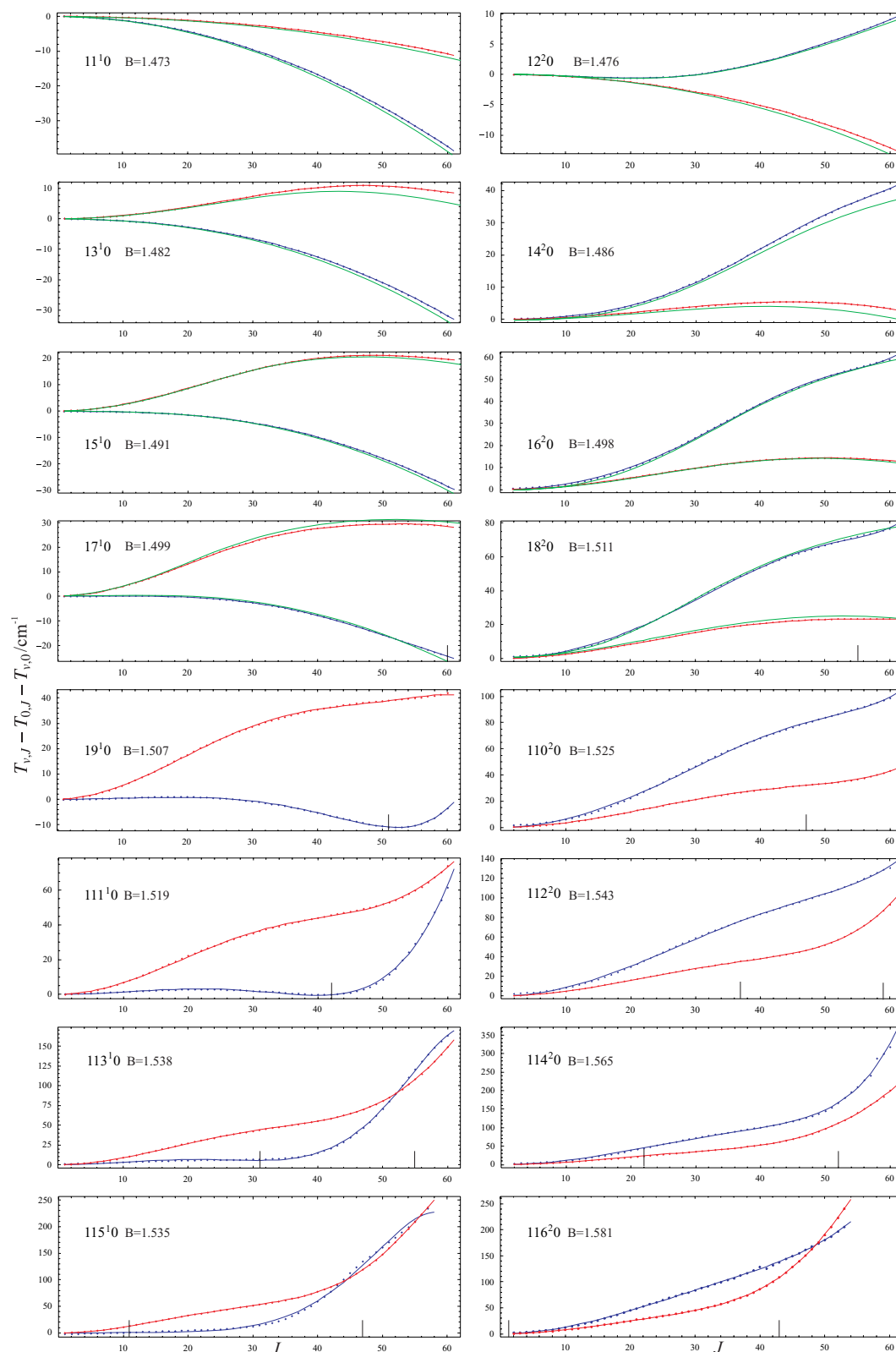
FIG. 8. The evolution of the reduced rovibrational eigenenergy for the HCN $1\nu_2 0$ bending states up to the isomerisation barrier. The $E_{v,(J=0)}$ vibrational energy used to calculate the reduced energy was calculated from the *ab initio* data. (blue: e states; red: f states; green: experimental eigenenergies relative to the experimental $E_{v,(J=0)}$ vibrational energy; first vertical line: barrier height mark; second vertical line: barrier height plus $3300\ \mathrm{cm}^{-1}$).

of the rotational structure with increasing bending excitation (for the vibrational assignment see Refs. 16). Figure 8 shows the step by step evolution of the rotational structure with increasing bending excitation for the $1v_20$ states. The rotational structure of the experimental and the *ab initio* data match perfectly within the resolution of the data plots.

IV. SATURATION OF THE HCN AND HNC ROVIBRATIONAL STATES WITH HIGH ANGULAR MOMENTUM

Figure 4 shows the evolution of the rovibrational eigenenergy with maximum angular momentum $l = v_2$. Classically, the $l = v_2$ case corresponds to the situation of nuclei rotating around the molecule axis. The HCN eigenenergy structure reaches a limit for $v_2 = 8$. For the vibrational states with $v_2 > 8$ the rotational eigenenergy structure does not change any more, the molecule is "locked" on the molecular axis. For HNC there is a change in the eigenenergy structure for $v_2 \geq 7$ to lower eigenenergy values. This happens due to the slope change in the potential surface as shown in the inset in Fig. 4.

For the high l states the *ab initio* data insets in Fig. 4 perfectly reproduce the measured eigenenergy structure up to $v_2 = 11$. Figure 5 shows the evolution of the $l = v_2$ bending states for $v_2 > 11$. From the *ab initio* data we can see that a structure change begins to take place at approximately half the barrier height ($v_2 = 11$). The vibrational energy begins to accommodate to the levels above the barrier mainly at high vibrational excitations of $v_2 > 22$ just above the barrier[16] first only for low l states, the high l states remain linear HCN states.[27] It is possible to argue that the rotational structure already experiences the influence of the barrier at much lower energies than the vibrational one. To understand the observed structural change at high l it is necessary to repeat the analysis presented here for similar isomerising linear molecules with different barrier heights and compare the obtained results.

V. CONCLUSION AND OUTLOOK

In this work we have shown that the rotational structure of HCN and HNC has an approximate twofold rotational degeneracy for low vibrational angular momentum and high rotational excitation until effects due to the isomerisation barrier spoil it. We have demonstrated using rotationally and vibrationally assigned *ab initio* calculations that the rotation states are much more sensitive to the isomerisation barrier than the vibrational states. The high vibrational angular momentum states begin to accommodate the eigenenergy structure already at rovibrational energies corresponding approximately to half the barrier height. For HNC the

experimental data demonstrates that the rotational eigenenergy structure is extremely sensitive to changes in the potential energy surface. Using the complete vibrational and rotational analysis for a triatomic molecule as an example it may now be much easier to search for alternative methods in solving the Schrödinger equation for polyatomic molecules. Using the findings of this work it will be possible to assign experimental HOTGAME spectra with even higher vibrational and rotational excitation and give an exact quantum mechanical picture in the frequency domain for a basic chemical model reaction, the HCN⇌HNC isomerisation reaction.

[1] K. S. Exner and G. Ch. Mellau, Visualization of the asymmetric infinite square double well energy eigenstates, *Poster L13, 21st Conference on H.R.M.S., Poznan* (2010).

[2] T. van Mourik, G. J. Harris, O. L. Polyanski, J. Tennyson, A. G. Császár, and P. J. Knowles, J. Chem. Phys. **115**, 3706 (2001).

[3] J. M. Bowman, Science **290**, 724 (2000).

[4] P. F. Bernath, Chem. Soc. Rev. **25**, 111 (1996).

[5] G. Ch. Mellau, J. Chem. Phys. **133**, 164303 (2010).

[6] S. N. Mikhailenko, Vl. G. Tyuterev, and G. Ch. Mellau, J. Mol. Spectrosc. **217**, 195 (2003).

[7] G. Ch. Mellau, S. N. Mikhailenko, E. N. Starikova, S. A. Tashkun, H. Over, and Vl. G. Tyuterev, gion, J. Mol. Spectrosc. **224**, 32 (2004).

[8] S. N. Mikhailenko, G. Ch. Mellau, E. N. Starikova, S. A. Tashkun, and Vl. G. Tyuterev, Actra, J. Mol. Spectrosc. **233**, 32 (2005).

[9] W. Quapp, M. Hirsch, G. Ch. Mellau, S. Klee, M. Winnewisser, and A. Maki, Cli J. Mol. Spectrosc. **195**, 284 (1999).

[10] A. G. Maki, G. Ch. Mellau, S. Klee, M. Winnewisser, and W. Quapp, Hi, J. Mol. Spectrosc. **202**, 67 (2000).

[11] W. Quapp, V. Melnikov, and G. Ch. Mellau, J. Mol. Spectrosc. **211**, 189 (2002).

[12] G. Ch. Mellau, B. P. Winnewisser, and M. Winnewisser, J. Mol. Spectrosc. **249**, 23 (2008).

[13] J. P. Hofmann, B. Eifert, and G. Ch. Mellau, J. Mol. Spectrosc. **262**, 75 (2010).

[14] A. Maki and G. Ch. Mellau, J. Mol. Spectrosc. **206**, 47 (2001).

[15] G. Ch. Mellau, J. Mol. Spectrosc. **264**, 2 (2010).

[16] G. Ch. Mellau, "Complete experimental rovibrational eigenenergies of HCN up to 6880 cm^{-1} above the ground state," J. Chem. Phys. (submitted).

[17] G. C. Mellau, "The ν_1 band system of HCN," J. Mol. Spectrosc. (2011) (submitted).

[18] See supplementary material at http://dx.doi.org/10.1063/1.3590026 for the experimental and calculated rovibrational eigenenergies of HCN and HNC reported for the first time in this work.

[19] W. Gordy, and R. L. Cook, *Microwave Molecular Spectra*, 2nd Ed. (Wiley-Interscience, New York, 1984).

[20] J. K. G. Watson, High-ordelecules, J. Mol. Spectrosc. **1983**, 83 (1983).

[21] J. K. G. Watson, Can. J. Phys. **79**, 521 (2001).

[22] J. K. G. Watson, M. Herman, J. C. Van Craen, and R. Colin, J. Mol. Spectrosc. **95**, 101 (1982).

[23] T. Hirano, V. Derpmann, U. Nagashima, and P. Jensen, - J. Mol. Spectrosc. **263**, 150 (2010).

[24] G. J. Harris, O. L. Polyanski, and J. Tennyson, Astrophys. J. **578**, 657 (2002).

[25] G. J. Harris, J. Tennyson, B. M. Kaminsky, Y. V. Pavlenko, and H. R. A. Jones, Mon. Not. R. Astron. Soc. **367**, 400 (2006).

[26] J. M. Bowman, S. Irle, K. Morokuma, and A. Wodtke, J. Chem. Phys. **114**, 7923 (2001).

[27] K. Efstathiou, M. Joyeux, and D. A. Sadovskii, Phys. Rev. A **69**, 032504 (2004).